JOURNAL OF MATERIALS SCIENCE 39 (2004) 961–968

Changes in the physicochemical and optical properties of chalcogenide thin films from the systems As–S and As–S–Tl

K. PETKOV, R. TODOROV, D. KOZHUHAROVA
Central Laboratory of Photoprocesses, Bulgarian Academy of Sciences, Acad. G. Bonchev St., bl. 109, 1113 Sofia, Bulgaria

L. TICHY, E. CERNOSKOVA
Joint Laboratory of Solid State Chemistry of Institute of Macromolecular Chemistry of Czech Academy of Science and University of Pardubice, Studentska 84, 53009 Pardubice, Czech Republic

P. J. S. EWEN
School of Engineering and Electronics, University of Edinburgh, Edinburgh EH9 3JL, UK

Changes in some physical and optical properties of thermally evaporated thin films from the systems As–S and As–S–Tl over a wide range of concentrations have been investigated. The influence of the conditions of vacuum deposition and light exposure has been demonstrated. The optical transmission and reflection of thin layers deposited on BK-7 optical substrates have been measured in the spectral region of 350–2000 nm and the linear (n) and nonlinear (n_2) refractive indices and optical band-gap, E_g, as well as the oscillator fitting constants, were calculated. Boling's formula is used to predict n_2 from the dispersion and the magnitude of n. Data for changes in the glass-transition temperature, T_g, microhardness, and rate of dry etching of thin chalcogenide films before and after exposure to light are presented. The addition of Tl in As_2S_3 leads to an increase in the refractive index and decrease in the optical band-gap. After illumination a photodarkening or photobleaching effect was observed depending on the evaporation conditions. Some of the layers change their etching rate in a plasma which make them suitable for practical applications. Conclusions on the homogeneity of the layers and the origin of photostructural changes in them are drawn.

1. Introduction

Amorphous chalcogenides are typical non-crystalline semiconductors exhibiting metastable phenomena and they have been extensively studied for several decades because of their interesting fundamental properties and because of their potential applications in optical imaging, optical recording, infrared and integrated optics, microelectronics and optical communications. Amorphous chalcogenide films are very promising for nano-technology, for photosensitive photo-recording and as radiation sensitive materials with very high optical resolution and very good optical properties. Most of these applications are based on the wide variety of light-induced effects exhibited by these materials [1–4]. Although the properties of glass-forming systems such as As–S, As–Se, Ge–Se and Ge–S have been extensively studied, there is insufficient information for more complex multi-component systems. Photostructural changes result in a change in the solubility rate of some chalcogenides [5, 6], making them more soluble after illumination in alkaline solutions. The interest in chemical dry etching has grown considerably in recent years due to its advantages over wet etching [7, 8].

Arsenic chalcogenide glasses are of great interest in bulk infrared optics because of their good infrared transmission and extensive glass-forming tendency [9–11]. Addition of network formers or modifiers is expected to change the properties of glasses and widen the scope of their applications. In our previous investigations [12–15] of the changes in the dissolution rate and the optical properties of thin As–S–Tl (Bi), As–Ge–S and Ge–S–Bi films we have drawn some conclusions on their practical application.

The addition of some metals to the chalcogenide glasses from the systems As–S and Ge–S influences their optical and electrical properties. It seems there is a special interest in the investigation of changes caused when thallium is used for this purpose. In several papers where a very complicated system As_2S_3–Tl_2S–Sb_2S_3 has been studied [11, 16, 17], some data for the shift of absorption edge, band-gap and structure depending on Tl content in the binary As_2S_3–Tl_2S system are presented.

More recently, significant interest has arisen in the non-linear optical properties of chalcogenide glasses because of their potential use in optical switching devices [18, 19]. The experimental determination of the optical nonlinear response of a material usually requires an elaborate measuring technique such as Z-scan, four wave mixing or optical third-harmonic generation [20, 21]. However, semi-empirical formulae have been developed [22] to predict n_2 for various glasses and crystals with accuracy similar to that of the measurements mentioned above.

The aim of this work is to present some results on the optical, thermal and mechanical properties, as well as on changes in the dry etching rate, of thin As–S and As–S–Tl films, depending on the film composition. Some comments on the influence of the conditions of their deposition on the homogeneity of the coatings will be made. Conclusions for their practical application based on the changes that occur in their dry etching rate after exposure will be made.

2. Theory

The refractive index, n, and the film thickness were calculated using Swanepoel's method [23] and a computer program developed by Konstantinov [24]. The method allows the calculation of n when both the refractive index of the substrate and the position of the interference extrema are known. In the present work the refractive index, s, of the substrate was determined independently at various wavelengths by measuring the transmittance, T_s, of the substrate alone and using the equation [24]:

$$s = 1/T_s + 1/\left(T_s^2 - 1\right)^{1/2}. \tag{1}$$

For BK-7 glass substrates it was found that $91 \leq T_s \leq 92$ and $89 \leq T_s \leq 91$ over the wavelength ranges 350–1400 and 1400–2500 nm, respectively. The program used to calculate n will determine it to an accuracy of $\pm 0.5\%$ for an error in the transmittance of $\pm 0.1\%$.

For chalcogenide semiconductors, the optical absorption coefficient, α, changes rapidly for photon energies comparable to that of the band-gap, E_g, giving rise to an absorption edge with three regions—one at high electron energies, one in the region of the edge itself ($10 < \alpha < 10^4$ cm^{-1}), and one at the lowest photon energies [4]. The first is for the highest values of the absorption coefficient ($\alpha \geq 10^4$ cm^{-1}) which corresponds to transitions between extended states in both valence and conduction bands where Tauc's power law is valid [25]:

$$\alpha h\nu = B(h\nu - E_g)^2. \tag{2}$$

B is the slope of the Tauc edge, which reflects some disorder of the samples. Usually this constant depends on the width of the localized states in the band-gap, which are attributed to the homopolar bonds in the chalcogenide glasses. Thus, Tauc's plots of $(\alpha h\nu)^{1/2}$ versus $(h\nu)$ should be linear and extrapolate to values of the optical gap, E_g.

In the third region, the absorption coefficient exhibits an exponential behaviour

$$\alpha = \alpha_0 \exp(h\nu)/E_e \tag{3}$$

The absorption in this region is due to transitions between extended states in one band and localized states in the exponential tail of the other band. E_e is connected with the width of the more extended band tail and it is often called the Urbach energy. It is determined by the degree of disorder in the amorphous chalcogenides.

The refractive index dispersion $n(h\nu)$ of amorphous materials can be fitted by the Wemple-DiDomenico relation [26, 27]

$$n^2 - 1 = E_d E_o/\left(E_o^2 - h^2\nu^2\right), \tag{4}$$

where E_o is the oscillator energy and E_d is the dispersion energy. By plotting $(n^2 - 1)^{-1}$ against $(h\nu)^2$ and fitting a straight line, E_d and E_o can be directly determined from the slope, $(E_d E_o)^{-1}$, and the intercept E_o/E_d on the vertical axis. The macroscopic oscillator strength E_d is related to the cation coordination number, anion valency, and ionicity by

$$E_d = f n_e Z_a (N_A d^3), \tag{5}$$

where n_e is the number of valence electrons per anion (usually $n_e = 8$), Z_a is the anion valence (2 for oxides, 1 for fluorides), and N_A is the anion number density. The normalized oscillator strength f for crystals and glasses is unaffected by disorder. This indicates that the bond lengths remain essentially unaltered and illustrates the insensitivity of bond-dependent optical properties to the absence of long-range order.

3. Experimental

Glasses were prepared by direct synthesis from the elements with a purity of 99.999%. These were heated in an evacuated silica ampoule placed in an oven at 700°C for 12 h with subsequent cooling in cold water. In order to achieve good homogenization of the chalcogenide glasses the oven was slowly rocked during the time the ampoule was at high temperature. Thin films were deposited at room temperature onto soda-lime glass, Si and BK-7 optical glass substrates by thermal evaporation of previously weighed powdered glassy material or by evaporation from a larger quantity and stopping the process when the thickness needed is reached. For determination of the optical homogeneity of thin As–S films some experiments were made on thin layers (about 80 nm thick) which were deposited consecutively in the same vacuum cycle and on a layer whose thickness represents the sum of the thicknesses of these thin layers. The films were exposed to light from a halogen lamp with an intensity of 20 mW · cm^{-2} or by a mercury high-pressure lamp (ORIEL-200 W) at intensity 120 mW · cm^{-2}. The composition of both bulk glasses and thin films was determined in a scanning electron microscope with an X-ray microanalyzer (Jeol Superprobe 733). Optical transmittance and reflectivity

measurements were carried out using a Perkin Elmer Lambda 9 or a Carry 5E UV-VIS-NIR Spectrophotometer. The ellipsometric measurements were carried out at three angles of light incidence in the interval 45–55°, at $\lambda = 632.8$ nm, using MAI-ellipsometry. A modified commercial vacuum installation HZM-4 was used for dry etching. The diode electrode configuration was connected to a 2.56 MHz high frequency power supply. The rf power density was varied in the range 50–350 $mW \cdot cm^{-2}$. The experiments were mainly performed at a pressure $p = 8$–10 Pa and a power density of 130 $mW \cdot cm^{-2}$.

4. Experimental results

4.1. Glass synthesis and thermal properties

Conditions for the synthesis of As-containing glasses with specific compositions have been established. The result of the X-ray microanalysis performed (Table I) showed that the compositions of bulk samples as well as of evaporated layers are very close to the expected ones. The bulk samples were subjected to X-ray and electron diffraction analysis, which confirmed that only the amorphous phase is present (only $As_{45}S_{55}$ glass contained traces of a crystalline phase—the molecular crystal As_4S_4).

DSC was used to determine the glass-transition temperature, T_g, of both bulk glasses and thin As—S—Tl films by using 50 mg of samples in powdered form (thin films were scratched from the substrates) and a heating rate of 20 $K \cdot min^{-1}$. The Knoop hardness H of thin amorphous films (1 μm thick) was determined using a load of 3.5 g to produce an impression on each specimen. The length of the diagonal for each square impression on the surface was measured. It was shown (Fig. 1a) that T_g decreases for both bulk glasses and thin layers on increasing the Tl content, which correlates with changes in the microhardness (Fig. 1b) of these samples. Neither the glass-transition temperature nor the microhardness of the layers depends on the conditions of the film deposition (temperature of evaporation and the quantity of the material in the boat). After exposure the values of the microhardness increase by 20–30% owing to structural changes in the layers after illumination. More details from these experiments will be presented elsewhere.

TABLE I Composition obtained from X-ray microanalysis for bulks and thin films investigated

Composition	Expected composition	Obtained compositions	
		Bulk samples	Thin films
As_1S_9	$As_{10}S_{90}$	$As_{15}S_{85}$	$As_{20}S_{80}$
As_2S_5	$As_{28}S_{72}$	$As_{29.7}S_{70.3}$	$As_{28.5}S_{71.5}$
As_2S_4	$As_{33}S_{67}$	$As_{33.8}S_{66.2}$	$As_{33.6}S_{66.4}$
$As_{38}S_{62}$	$As_{38}S_{62}$	$As_{38}S_{62}$	$As_{38}S_{62}$
As_2S_3	$As_{40}S_{60}$	$As_{39.1}S_{60.9}$	$As_{41}S_{59}$
$As_{42}S_{58}$	$As_{42}S_{58}$	$As_{43}S_{57}$	$As_{42}S_{58}$
$As_{45}S_{55}$	$As_{45}S_{55}$	$As_{43.3}S_{56.7}$	$As_{45}S_{55}$
$(As_2S_3)_{97}Tl_3$	$As_{39}S_{58}Tl_3$	$As_{38.8}S_{59.5}Tl_{1.7}$	$As_{43}S_{54.6}Tl_{2.4}$
$(As_2S_3)_{94}Tl_6$	$As_{38}S_{56}Tl_6$	$As_{37}S_{57}Tl_6$	$As_{41}S_{54}Tl_5$
$(As_2S_3)_{90}Tl_{10}$	$As_{36}S_{54}Tl_{10}$	$As_{37.8}S_{53.5}Tl_{8.7}$	$As_{34}S_{53}Tl_{13}$

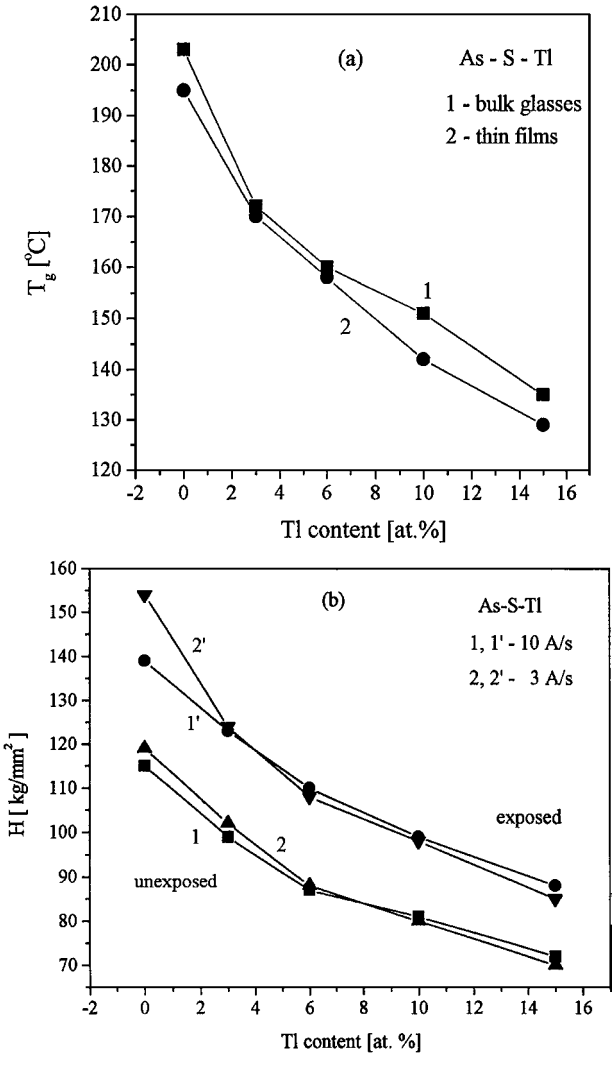

Figure 1 Compositional dependence of the glass forming temperature, T_g, of bulks and thin films (a) and microhardness of thin films deposited at two rates of evaporation (b) from the system As—S—Tl.

4.2. Optical properties

We synthesized chalcogenide glasses with the following compositions As_xS_{100-x} $(10 \leq x \leq 45)$ and $(As_{40}S_{60})_{100-x}Tl_x$ $(0 \leq x \leq 10)$. The optical transmission of unexposed and exposed thin films (1 μm thick) was measured by an UV-VIS-IR spectrophotometer and the linear (n) and nonlinear (n_2) refractive indices of unexposed and exposed thin films as well as the band-gap, E_g and the oscillator fitting constants were determined. The exposure time to saturation was experimentally established for all compositions.

Table II shows the experimental data for n (at $\lambda = 656.2$ nm), E_g, E_d, E_o and n_2 for thin As—S films. The shift of the absorption edge, $\Delta\lambda$, the refractive index, n, for unexposed and exposed films and Δd from the transmission measurements of thin As_xS_{100-x} $(28 \leq x \leq 45)$ are shown in Table III. The calculated values of the refractive index of unexposed As—S films are in good agreement with the results published in the literature [27]. The refractive index as well as the absorption edge shift increase with increasing As content in the films and pass through a maximum for the stoichiometric composition $As_{40}S_{60}$ (or $As_{42}S_{58}$) (Fig. 2). After exposure to light, n and the compactness of the layers increase (for $As_{40}S_{60} - \Delta\lambda = 10$ nm ($T = 20\%$),

TABLE II Linear and nonlinear optical parameters for thin As–S

	n_c		E_g		E_d		E_o		n_2	
Composition	Unexp	Exp	Unexp	Exp	Unexp	Exp	Unexp	Exp	Unexp	Exp
$As_{10}S_{90}$	2.17	2.23	2.68	2.64	16.7	18.4	5.22	5.41	101	93
$As_{28}S_{72}$	2.34	2.36	2.53	2.54	19.5	19.5	5.07	5.00	155	172
$As_{33}S_{67}$	2.41	2.51	2.49	2.47	20.8	21.7	5.07	4.88	162	224
$As_{38}S_{62}$	2.45	2.56	2.42	2.41	21.4	21.8	5.04	4.73	182	268
$As_{40}S_{60}$	2.45	2.55	2.39	2.38	21.3	22.1	5.03	4.81	197	266
$As_{42}S_{58}$	2.46	2.57	2.35	2.34	21.1	22.5	4.91	4.81	216	291
$As_{45}S_{55}$	2.44	2.54	2.33	2.32	20.9	21.2	4.97	4.67	182	285

TABLE III Experimentally obtained values of $\Delta\lambda$, n ($\lambda = 632.8$ nm) for unexposed and exposed thin As–S films

Composition	$\Delta\lambda$ (nm) ($T = 20\%$)	$n_{unexp.}$	$n_{exp.}$	Δn	Δd (nm)
$As_{40}S_{60}$	+10	2.44	2.56	+0.12	−8
$As_{28}S_{72}$	+4	2.33	2.40	+0.07	−15
$As_{33}S_{67}$	+5	2.43	2.50	+0.07	−11
$As_{45}S_{55}$	+9	2.43	2.52	+0.09	−9

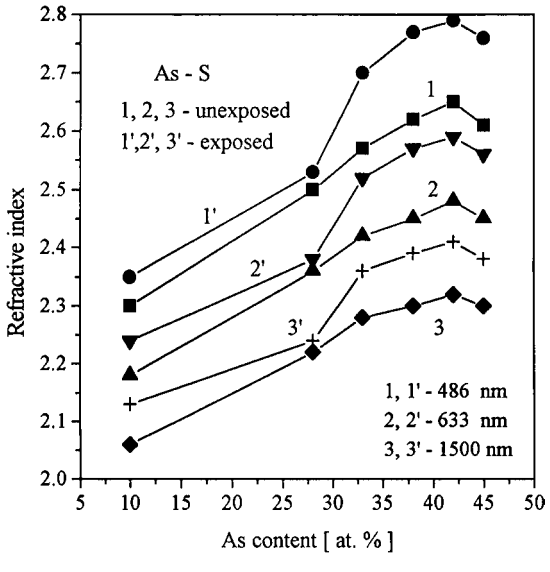

Figure 2 Compositional dependence of the refractive index, n, for unexposed and exposed As—S films.

$\Delta n = 0.12$ at $\lambda = 632.8$ nm and $\Delta d = -8$ nm). The same dependence for n, d and $\Delta\lambda$ was observed when the calculation was made from ellipsometric measurements and using double and triple spectrophotometric methods [29]. The thickness of the layers does not influence the optical properties of the As–S coatings. The ellipsometric measurements under different angles of incidence of the light show that all As–S coatings are homogeneous in thickness.

The absorption coefficient, α, calculated from Equation 1 shows a linear dependence in the region of high absorption. The band-gap determined from the plots $(\alpha h\nu)^{1/2}$ vs. $(h\nu)$ decreases with increasing the As content of the films (from 2.68 eV for $As_{10}S_{90}$ to 2.33 eV for $As_{45}S_{55}$) (Fig. 3a). For S enriched thin films the quantity of S–S bonds, which are longer than As–As ones, increase. That leads to an increase of the average length and to an increase in the band-gap. After illumination E_g decreases for all the compositions investigated (Fig. 3b) and the factor B increases (for example—from 795 $cm^{-1/2}$ $eV^{-1/2}$ for as-deposited to 876 $cm^{-1/2}$ $eV^{-1/2}$—for the exposed). According to Mott and Davis [28] the changes in B could be connected with the creation of the localized states at the edges of the conduction and valence bands.

Thin films (1000 nm thick) from the system As–S–Tl were deposited by thermal evaporation

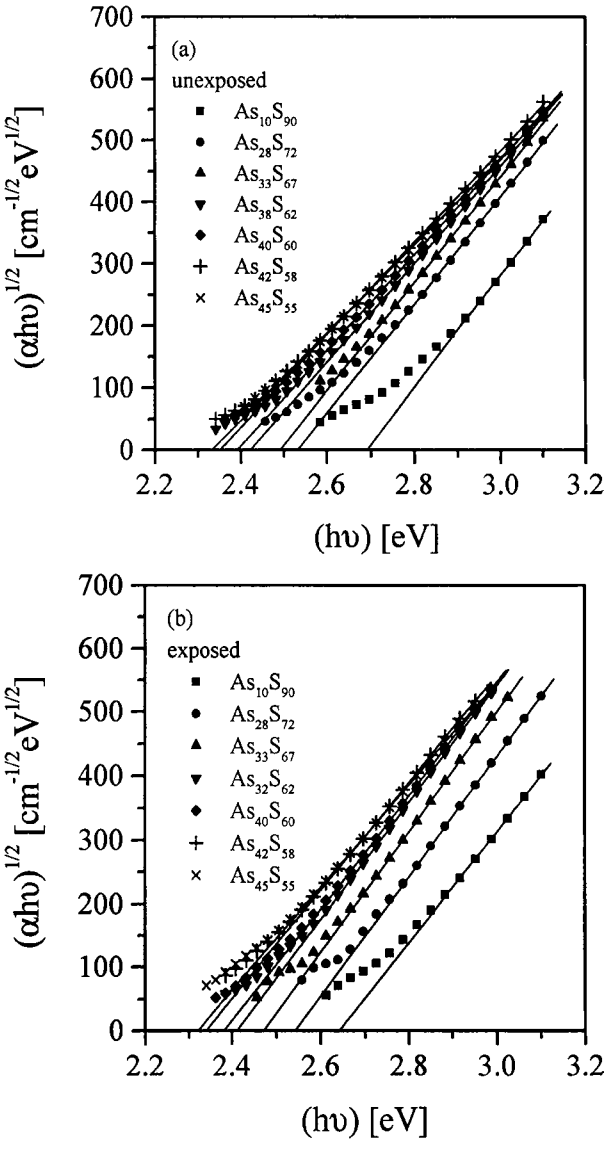

Figure 3 Optical absorption edge $(\alpha h\nu)^{1/2}$ vs. energy of photon $(h\nu)$ for unexposed (a) and exposed (b) thin As—S films.

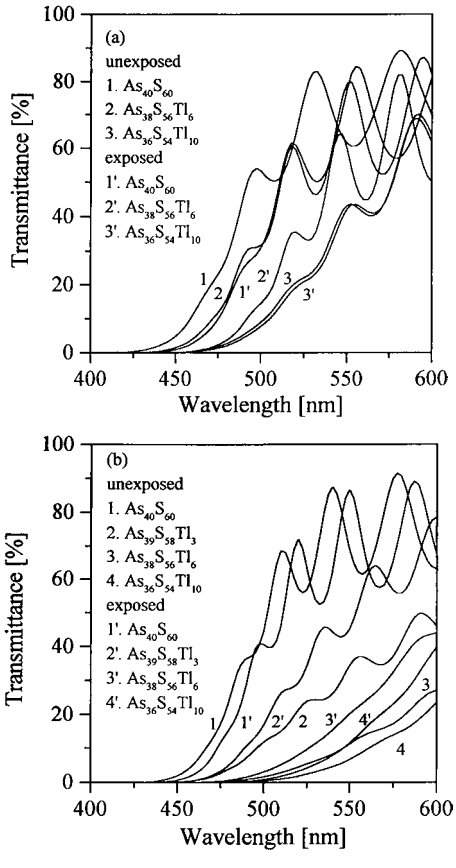

Figure 4 Optical transmission of unexposed thin As—S—Tl films deposited by thermal evaporation with (a) and without (b) residual in the boat.

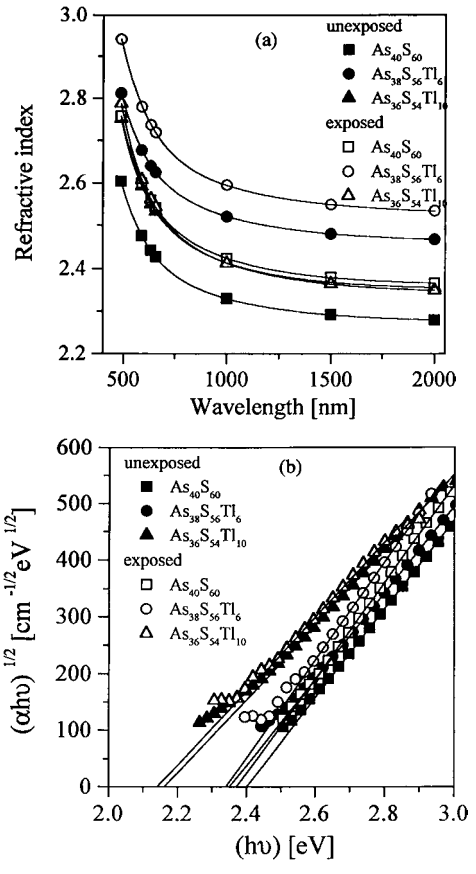

Figure 5 Refractive index, n, (a) and optical absorption edge $(\alpha h\upsilon)^{1/2}$ (b) vs. wavelength, λ, for unexposed and exposed thin As—S—Tl films.

(with and without a residual in the boat after film deposition) of powdered bulk glasses with compositions $As_{39}S_{58}Tl_3$, $As_{38}S_{56}Tl_6$ and $As_{36}S_{54}Tl_{10}$ [29]. As is seen from Fig. 4, the absorption edge of unexposed thin films was shifted to longer wavelengths on increasing the Tl content in As_2S_3. After exposure to light a photodarkening effect occurred for the layers deposited with a residual in the boat while photobleaching is observed for the layers deposited, when an exact quantity of the bulk glassy substance was evaporated for the expected film thickness. The largest value of the shift of the absorption edge, $\Delta\lambda = +42$ nm, was found for thin $As_{38}S_{56}Tl_6$ films. For the same composition, a maximum change in the refractive index after exposure to light was observed ($\Delta n = 0.16$) (Fig. 5a). For as-deposited As—S—Tl films the optical band-gap decreases from 2.39 eV for $As_{40}S_{60}$ to 2.16 eV for thin $As_{36}S_{54}Tl_{10}$ films (Fig. 5b). At the same time the slope of the absorption coefficient decreases because of a decrease in the disordering. As principally, for the glass system As—S—Tl the value of E_g decreases with increasing Tl content, we believe that in the process of absorption the incident photon excites electrons from states near the top of the valence band to states near the bottom of the conduction band, i.e., across the pseudogap. For a better understanding of these changes some IR measurements were made and the results will be published later.

For estimation of the optical homogeneity in the volume of thin layers, the transmittance of thin films (about 80 nm thick) which were deposited consecutively in the same vacuum cycle together with a layer whose thickness represents the sum of the thicknesses of these coatings, was measured and the values of n were calculated. Fig. 6 represents the dependence of the refractive index, n, on the serial number of the layers for unexposed (Fig. 6a and c) and exposed (Fig. 6b and d) thin As—S and As—S—Tl layers using some double and triple methods described in [29]. All samples were deposited by evaporation of the whole quantity of the glass substance, i.e., without any residue in the boat. It is seen that the refractive index for as-deposited As—S films does not changes with the serial number, while n considerably increases for the last two numbers of the system As—S—Tl. After exposure n decreases, i.e., a photobleaching is observed. That means the As—S thin films are homogeneous in their thickness while during the process of vacuum deposition of As—S—Tl coatings, a process of decomposition takes place.

4.3. Nonlinear refractive index

Research into nonlinear optical materials has recently been stimulated by the future need for nonlinear optical devices. Third-harmonic generation measurement is often used in the search for new nonlinear materials. It was found that As_2S_3 chalcogenide glass has 300 times larger $\chi^{(3)}$ compared with the silica glass [30]. Using a semi-classical model of the simple harmonic oscillator Boling *et al.* [22] first derived a relation between the non-linear refractive index, n_2, the resonance frequency, ω_0, and the product NS (N is the density of polarizable ions and S is the oscillator

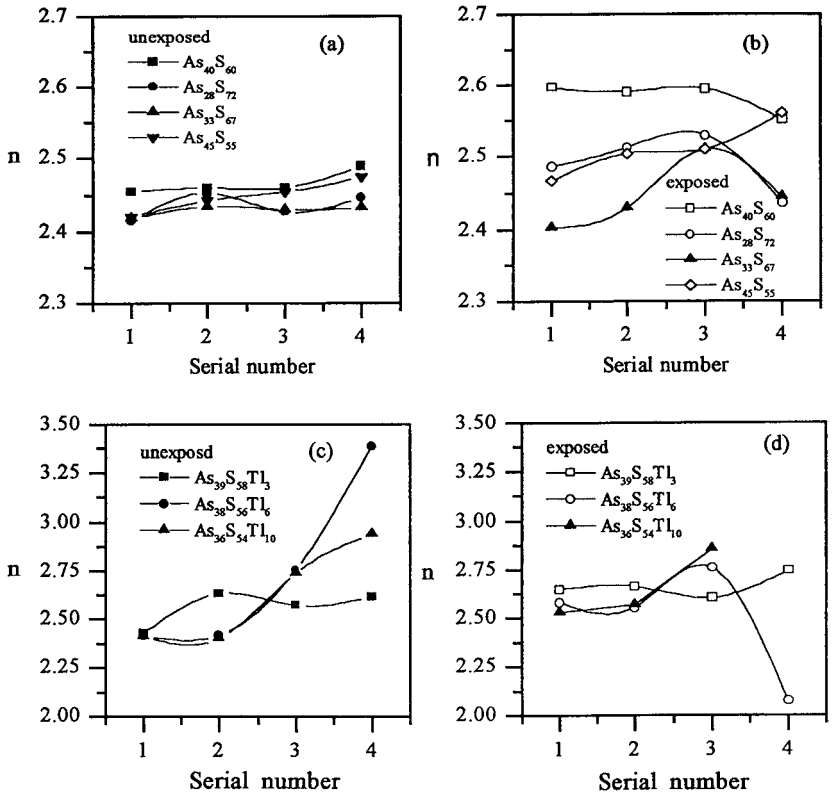

Figure 6 Changes in the refractive index, n, depending on the serial number of vacuum deposited As—S (a, b) and As—S—Tl (c, d) films.

strength). They showed how ω_0 and NS could be related to the parameters namely n_d and Abbe number, ν_d: $\nu_d = (n_d - 1)/(n_f - n_c)$, where n_d, n_f and n_c are the linear refractive indices at the following standard wavelengths $\lambda_f = 486.13$ nm, $\lambda_d = 587.56$ nm and $\lambda_c = 656.27$ nm.

Two formulae derived by Biling *et al.* [22]

$$n_2(10^{-13}\text{esu}) = 68(n_d - 1)\left(n_d^2 + 2\right)^2 \Big/ \nu_d \Big\{1.517 + \left[\left(n_d^2 + 2\right)(n_d + 1)\nu_d\right] \Big/ 6n_d \Big\}^{1/2} \quad (6)$$

and

$$n_2(10^{-13}\text{esu}) = 391(n_d - 1)/\nu_d^{5/4} \quad (7)$$

could be used for prediction of n_2 to an accuracy of ~20% or better using the values of the linear refractive index, n. In the case of IR-transmitting glasses such as the chalcogenides, parameters such ν_d and n_d may not be appropriate for expressing their dispersion relations because they are relatively absorbing in the visible. A better approach might be to fit the complete dispersion curves of these materials using the Wemple-Di Domenico model [26] and then to express Boling's formula (6). Using the parameters E_o, the oscillator energy, and E_d, the dispersion energy, we have presented [15] data for some chalcogenide films using the following expression for n_2:

$$n_2 = 3^{0.5} gS(n^2+2)^{1.5}(n^2-1)^2 h^2 e^2 / 12\,\text{nm}\, E_d E_o^2, \quad (8)$$

where n is the linear refractive index at long wavelengths, S—the oscillator strength, h is Planck's constant divided by 2π, g is the anharmonicity parameter, e and m are the electron charge and mass respectively.

In Table II, the values of n_2 before and after exposure of thin As—S films are compared (using (6) while in Table IV the comparison is for thin As—S—Tl layers. It is found that n_2 increases with increasing the As content in the films (unexposed and exposed) passing through maximum for the composition $As_{42}S_{58}$. This correlates with the data obtained for n_c. The nonlinear refractive index for unexposed thin As—S—Tl films increases with increasing Tl content in films passing through minimum for the composition $As_{39}S_{58}Tl_3$ which correlates with the changes in the linear refractive index. After illumination n_2 increases and the biggest change is for the same composition.

4.4. Dry etching

Studies carried out earlier [5] on films make it possible to obtain masks and gratings with submicron structures in those films using a wet etching method (alkaline solvents with surfactants). The use of dry etching for making a relief in chalcogenide thin films could solve

TABLE IV Values of n, E_g and n_2 for unexposed and exposed thin As—S—Tl films, deposited with (1) and without (2) residue in the boat

	n_c (1)		n_c (2)		E_g		n_2	
Composition	Unexp	Exp	Unexp	Exp	Unexp	Exp	Unexp	Exp
$As_{40}S_{60}$	2.45	2.55	2.45	2.55	2.39	2.37	197	266
$As_{39}S_{58}Tl_3$	2.41	2.52	2.70	2.66	2.38	2.37	164	291
$As_{38}S_{56}Tl_6$	2.63	2.72	2.62	2.49	2.35	2.34	184	273
$As_{36}S_{54}Tl_{10}$	2.53	2.54	2.59	2.44	2.16	2.14	257	265

TABLE V Dry etching rates of unexposed and exposed thin chalcogenide films and bulks in CCl_2F_2 plasma: pressure—8–10 Pa; rf power density—130 mW cm^{-2}; etching time—120 s

Compositions	Etching rate of unexposed samples (nm/s)	Etching rate of exposed samples (nm/s)
$As_{45}S_{55}$	5.0	7.5
$As_{40}S_{60}$	6.5	5.5
$As_{33}S_{67}$	7.5	7.5
$As_{28}S_{72}$	6.2	5.5
$(As_2S_3)_{97}Tl_3$	2.3	5.2
$(As_2S_3)_{94}Tl_6$	3.2	0
$(As_2S_3)_{90}Tl_{10}$	1.8	2.4
As_2S_3—bulk glass (5.0 μm etched)	2.4	
As_2S_4—bulk glass (5.0 μm etched)	1.8	
$Ge_{28}S_{66}Bi_6$	0.3	0
$(GeS_2)_{94}Bi_6$	1.2	0.6

some technological problems associated with producing deep structures in them by choosing suitable glass composition and optimizing the etching regime.

In this investigation we have studied the changes in the etching rate of unexposed and exposed thin layers (200 nm thick) from the systems As–S and As–S–Tl as well as thick $As_{40}S_{60}$ and $As_{33}S_{67}$ films (about 5 μm) and bulk glasses. Etching was carried out with different plasma power density using CCl_2F_2, Ar, dry air, and a mixture of Ar and CCl_2F_2. It was found that the etching rate of unexposed thin films from the system As–S–Tl depends very strongly on the composition while there is no big difference in the etching rate of thin As–S layers (Table V). The etching rate depends on etching time and the power density of the plasma and it was 2 times lower for etching of bulk glasses compared with the etching of 5.0 μm thick layers. Adding small quantities of Tl in the thin As_2S_3 layers makes them unetchable in CCl_2F_2 plasma. That means if we can produce photoinduced diffusion of Tl into thin As_2S_3 layers they could be used as an inorganic photoresist. All these changes could be associated with the photo-induced structural changes in the layers after light exposure (more information will be published elsewhere).

The best conditions for reaching the highest ratio between the etch rates are if the rf power is about 40 W (CCl_2F_2 plasma, 8×10^{-2} Torr, gas flow—15 ccm/min). When a mixture of CCl_2F_2 and Ar is used, the selectivity of the dry etching process diminishes. The etching rate of thin As_2S_3 films using CCl_2F_2 plasma was several times lower than that when CF_4 plasma was used [8].

5. Discussion

The as-deposited thin films from the system As_xS_{100-x} are a heterogeneous mixture of structural units of the type As_2S_3, As_4S_3, As_4S_4, As_4S_8, As_4, S_8 and contain some homopolar bonds (As–As, S–S). The presence of As_4S_4 molecules is responsible for the appearance of peaks at 375 and 336 cm^{-1} in the infrared spectra, and the AsS_3 pyramids for the peak at 310 cm^{-1}. In illumination, polymer destructive changes occur leading to the weakening of some bonds and to strengthening of others [31, 32]. The irreversible change occurring after exposure of as-deposited films are accompanied by a density increase of the As-S bonds, i.e., photopolymerization of As_4S_6 molecules. This leads to an increase in refractive index and considerable changes in the absorption peaks at 375 and 308 cm^{-1} obtained by infrared spectroscopy.

The structure of as-deposited films from the system As–S–Tl is more complicated because new structural units, such as $TlAsS_2$, Tl_3AsS_3 and others, are included. The existence of photoinduced structural changes in As–S–Tl chalcogenide films is supported by changes in their optical properties. The addition of Tl to arsenic sulfide leads to the increase in the refractive index and decrease in E_g and to creation of localized states in the band-gap. The addition of Tl to As_2S_3 results in a considerable decrease in the microhardness of thin films. After illumination it increases by 20%. This phenomenon could be explained by changes in the structure and the coordination number of layers.

As first suggested by Heo *et al.* [33] from the analysis of the core level X-ray photoelectron spectra the Tl atoms are expected to break some As–S–As bridges present in the As_2S_3 matrix and to lead to terminal As–S bonds and a creation of Tl–S bonds. Because of the more ionic character of the As–S bonds compared with the Tl–S bonds, two types of S atoms must be distinguished: the bridging sulfur atoms S_b occurring in As–S_b–As bridges and the non-bridging sulfur atoms in As–S_{nb}–Tl bridges [11]. The number of sulphur bridges As–S–As decreases and the number of non-bridging bonds As–S increases when the thallium concentration is raised. That means the addition of a small amount of Tl atoms to As_2S_3 strongly modifies the covalent network forming inhomogeneities in it or creating some covalent fragments linked by weak interactions which strongly modify both the optical band gap and the glass transition temperature. The short-range order is only slightly modified because of small Tl concentration in the samples.

6. Conclusions

Chalcogenide glasses from the systems As–S and As–S–Tl were synthesized and their element content has been determined. The bulk samples were subjected to X-ray and electron diffraction analysis, which confirmed that only amorphous phase is present (only $As_{45}S_{55}$ glass contained traces of a crystalline phase - As_4S_4 molecules). From the transmission and reflection measurements of thin As_xS_{100-x} ($10 \leq x \leq 45$) the optical constants, n, n_2 E_g, E_o and E_d have been determined and the influence of the composition and light illumination has been shown. It was shown that n, n_2, and E_d pass through a maximum for $As_{42}S_{58}$ which confirm the results published by Tanaka [27] and our previous results [5] for the maximum difference in the solubility of exposed and unexposed thin As–S films.

We have shown from the transmission measurements that both photodarkening ($\Delta\lambda = +42$ nm, at $T = 30\%$) and photobleaching ($\Delta\lambda = -32$ nm, at $T = 20\%$) occurred in the As–S–Tl layers after exposure to light depending on the conditions of evaporation. The

illumination causes a significant change in n and n_2 and an increase in the microhardness of the layers. A correlation between the compositional dependence of the microhardness and glass-transition temperature of glasses was found. The dry etch rate of thin As–S does not changes after exposure to light while the difference found for some As–S–Tl thin films give some potential to be used as high-resolution photoresist.

Acknowledgment

K. Petkov thanks the Royal Society for their financial support.

References

1. P. J. S. EWEN and A. E. OWEN, "High Performance Glases" (Blackie, London, 1992) p. 287.
2. G. PFEIFFER, M. A. PAESLER and S. C. AGARWAL, *J. Non-Cryst. Solids* **130** (1991) 111.
3. A. KOLOBOV and S. R. ELLIOTT, *Adv. Phys.* **40** (1991) 625.
4. S. R. ELLIOTT, in "Materials Science and Technology, A Comprehensive Treatment" (VCH, Weinheim, New York), "Glasses and Amorphous Materials" (1991) Vol. 9, p. 376.
5. K. PETKOV, M. SACHATCHIEVA and J. DIKOVA, *J. Non-Cryst. Solids* **101** (1988) 37.
6. K. PETKOV, M. SACHATCHIEVA and N. MALINOWSKI, *ibid.* **85** (1996) 309.
7. B. E. E. KASTENMEIER, P. J. MATSUO, J. J. BEULENS and G. S. OEHREIN, *J. Vac. Sci. Technol.* A **14** (1996) 2802.
8. E. HAITO, P. J. S. EWEN and A. E. OWEN, *J. Non-Cryst. Solids* **164/166** (1993) 901.
9. K. TANAKA, *Solid State Commun.* **34** (1980) 201.
10. A. B. SEDDON, *J. Non-Cryst. Solids* **184** (1995) 44.
11. P. E. LIPPENS, M. A. EL IDRISSI-RAGHNI, J. OLIVER-FOURCADE and J. C. JUMAS, *J. Alloys Compd.* **298** (2000) 47.
12. K. PETKOV, T. Z. ILIEV, R. TODOROV and D. TZVETKOV, *Vacuum* **58** (2000) 321.
13. K. PETKOV and B. DINEV, *J. Mater. Sci.* **29** (1994) 468.
14. K. PETKOV, P. J. S. EWEN and M. VLCEK, "Future Directions in Thin Film Science and Technology" (1996) p. 397.
15. K. PETKOV and P. J. S. EWEN, *J. Non-Cryst. Solids* **249** (1999) 150.
16. E. L. IDRISSI-RAGHNI, J.-M. DURAND, B. BONNET, L. HAFID, J. OLIVER-FOURCADE and J.-C. JUMAS, *J. Alloys and Compd.* **239** (1996) 8.
17. J.-M. DURAND, P. E. LIPPENS, J. OLIVER-FOURCADE, J.-C. JUMAS and M. WOMES, *J. Non-Cryst. Solids* **194** (1996) 109.
18. M. SHEIK-BAHAM, A. SAID, T. WAI, D. J. HAGAN and E. W. VAN STIVLAND, *IEEE J. Quantum Electron.* **26** (1990) 760.
19. H. NASU, Y. IBARA and K. KUBODERA, *J. Non-Cryst. Solids* **110** (1989) 229.
20. R. RANDEL-ROJO, T. KOSA, E. HAJTO, P. J. S. EWEN, A. E. OWEN, A. K. KAR and B. S. WHERRETT, *Opt. Commun.* **109** (1994) 145.
21. E. HAJTO, R. E. BELFORD, P. J. S. EWEN and A. E. OWEN, *J. Non-Cryst. Solids* **115** (1989) 29.
22. N. L. BOLING, A. J. GLASS and A. OWYOUNG, *IEEE J. Quantum Electron.* **QE-14** (1998) 601.
23. R. J. SWANEPOEL, *Phys.* E **16** (1983) 1214.
24. I. KONSTANTINOV, *Private Commun.*
25. J. TAUC, "Amorphous and Liquid Semiconductors" (Plenum Press, New York, 1974).
26. S. H. WEMPLE and M. DIDOMENICO, *Phys. Rev.* **B3** (1971) 1338.
27. K. E. TANAKA, *Thin Solid Films* **66** (1980) 271.
28. N. F. MOTT and E. A. DAVIS, "Electron Processes in Non-Crystalline Materials" (Mir, Moskow, 1982) p. 198.
29. R. TODOROV and K. PETKOV, *J. Optoelectron. Adv. Mater.* **3** (2001) 311.
30. K. KUBODERA, H. KANBARA and M. KOGA, *J. Appl. Phys.* **74** (1993) 3683.
31. K. PETKOV, M. VLCEK and M. FRUMAR, *J. Mater. Sci.* **27** (1992) 3281.
32. U. STORM and T. P. MARTIN, *Solid State Commun.* **29** (1979) 527.
33. J. HEO, J. S. SANGHERA and J. D. MAC-KENZIE, *J. Non-Cryst. Solids* **101** (1988) 23.
34. K. PETKOV, R. TODOROV, L. TICHY and P. J. S. EWEN, in Proceedings of the International Congress on Glass, Extended Abstracts (Edinburgh, UK, 2001) Vol. 2, p. 218.

Received 10 February
and accepted 12 September 2003